



IFSCC 2025 full paper (IFSCC2025-1340)

“Development of Plant Exosome Engineering for Multifunctional Skin Improvement and Anti-inflammatory.”

EUN JUNG KIM¹, SEO YEON PARK¹, EUN JU PARK*¹, JIN OH PARK¹, Won Jong Rhee²

¹Natural Products Laboratory, DAEBONGLS, INCHEON, Korea, South

²Division of Bioengineering, Incheon National University, Republic of Korea

1. Introduction

Plant-derived extracellular vesicles (EVs) have recently emerged as promising candidates in dermatological and cosmetic applications due to their functional diversity and biocompatibility. EVs are nanoscale vesicles, typically ranging from 50 to 150 nm in diameter, that facilitate intercellular communication by transporting proteins, nucleic acids, lipids, and carbohydrates in a membrane-enclosed structure. Compared to EVs derived from human cells or cell cultures, plant-derived EVs offer advantages including lower safety concerns, species-specific bioactivity, and high scalability without the need for bioreactor-based production systems.

In this study, EVs were isolated from red cabbage (*Brassica oleracea*), herein referred to as Rabex, using ultrafiltration followed by size exclusion chromatography. Rabex exhibited biological activity *in vitro*, promoting keratinocyte proliferation and exhibiting anti-inflammatory effects. These properties suggest its potential as a functional ingredient in cosmetic formulations designed for skin soothing, anti-aging, and sensitive skin care.

To enhance targeted cellular uptake and therapeutic efficacy, Rabex was further engineered by surface modification with hyaluronic acid (HA), a known ligand of the CD44 receptor. CD44 is highly expressed in keratinocytes and immune cells and is involved in skin barrier repair and hydration maintenance. The modified vesicles (t-Rabex) demonstrated increased delivery efficiency to both epidermal and immune cells, potentially improving their bioactivity in skin-related applications.

Collectively, these findings indicate that Rabex and its HA-engineered derivative t-Rabex may serve as effective plant-derived nanocarriers with potential utility in cosmetic applications aimed at improving skin health and function.

2. Materials and Methods

Isolation and Characterization of Plant-Derived Extracellular Vesicles

Extracellular vesicles (EVs), referred to as Rabex, were isolated from red cabbage (*Brassica oleracea* var. *capitata* F. *rubra*) cultivated in Korea. The plant tissues were homogenized, followed by differential centrifugation, ultrafiltration, and size exclusion chromatography (Izon Science, New Zealand) to obtain purified EVs. The size distribution and particle concentration were analyzed using nanoparticle tracking analysis (Nanosight NS300, Malvern, UK). Transmission electron microscopy (JEM-1010, JEOL, Japan) was used to confirm morphology, and zeta potential and polydispersity index (PDI) were measured using a Zetasizer Nano ZS (Malvern, UK).

Cell Culture and Uptake Analysis

Human keratinocyte-like Caco-2 cells and THP-1 monocytes (ATCC, USA) were cultured in MEM and RPMI-1640 medium (Corning, USA), respectively, supplemented with 10% fetal bovine serum (Gibco, USA) and 1% penicillin-streptomycin. Cells were maintained at 37°C in 5% CO₂.

Rabex was labeled with PKH67 (Sigma-Aldrich, USA) and incubated with cells for uptake analysis using confocal microscopy (Zeiss LSM, Germany) and flow cytometry (Beckman Coulter, USA). Nuclear staining was performed using Hoechst 33342 (Sigma-Aldrich, USA).

Evaluation of Skin-Relevant Bioactivity

To evaluate the cosmetic potential of Rabex, Caco-2 and THP-1 cells were treated with Rabex at concentrations ranging from 1×10^8 to 1×10^{11} particles/mL. Cell viability and proliferation were assessed using a WST-1 assay (Roche, Germany) after 96 h. To assess anti-inflammatory effects, THP-1 cells were differentiated into macrophage-like cells using PMA (200 ng/mL), followed by Rabex treatment and stimulation with LPS (250 ng/mL). Expression of TNF-α, IL-1β, and CD163 mRNA was measured by qRT-PCR.

Reactive oxygen species (ROS) levels were detected via DCF-DA staining (Sigma-Aldrich, USA) and fluorescence microscopy (Nikon Eclipse Ti2, Japan). Additionally, trypan blue exclusion was used to assess DSS-induced cytotoxicity in Caco-2 cells, and transepithelial electrical resistance (TEER) was measured using an EVOM2 voltohmometer (World Precision Instruments, France) to evaluate barrier function.

Engineering of Hyaluronic Acid-Conjugated Rabex (t-Rabex)

To enhance cell targeting, Rabex was surface-functionalized with hyaluronic acid (HA, 30–50 kDa) via DSPE-PEG2000-NH₂ conjugation using EDC/NHS chemistry. The resulting DSPE-PEG-HA was purified by dialysis (MWCO 2 kDa, Spectra/Por®, USA) and lyophilized. Successful conjugation was confirmed by ¹H-NMR (JEOL, Japan) and FTIR (Bruker, USA).

For surface modification, Rabex was incubated with DSPE–PEG–HA at 37°C for 4 h, followed by removal of unbound conjugate by ultrafiltration.

Targeted Delivery and CD44 Receptor Validation

To evaluate CD44-mediated targeting, Caco-2 and THP-1 cells were treated with PKH-labeled Rabex or t-Rabex. In some groups, THP-1 cells were pre-incubated with CD44-blocking antibodies (0.5 µg/mL; Cell Signaling Technology, USA). Uptake was quantified by flow cytometry and visualized by fluorescence microscopy.

3. Results

Isolation, Characterization, and Batch Consistency of Rabex

Rabex was successfully isolated from red cabbage juice using a sequential process involving ultrafiltration and size exclusion chromatography (SEC), allowing separation from protein contaminants. SEC analysis revealed that fractions 7 to 9 contained the highest concentration of particles, as confirmed by nanoparticle tracking analysis (NTA), which reported a mean diameter of 115.2 nm (Figure 1A). Protein contamination was minimal (Figure 1B), confirming high purity. Compared to mammalian cell-derived EVs, Rabex demonstrated dramatically lower production cost, supporting feasibility for large-scale applications.

Zeta potential and PDI measured by DLS showed typical EV characteristics: -14.1 mV and 0.25, respectively (Figure 1C). Stability analysis revealed that Rabex retained size and dispersion up to day 7 at both 2–8°C and 37°C, although a gradual decline in particle concentration was observed (Figure 1D). Furthermore, Rabex remained stable in 50% FBS regardless of temperature

Batch reproducibility was evaluated across three independent preparations over three years. TEM confirmed uniform spherical morphology (Figure 1E), and physicochemical parameters (size, zeta potential, concentration, yield) were consistent across all batches (Figure 1F). These findings validate Rabex as a reproducible and scalable vesicle material.

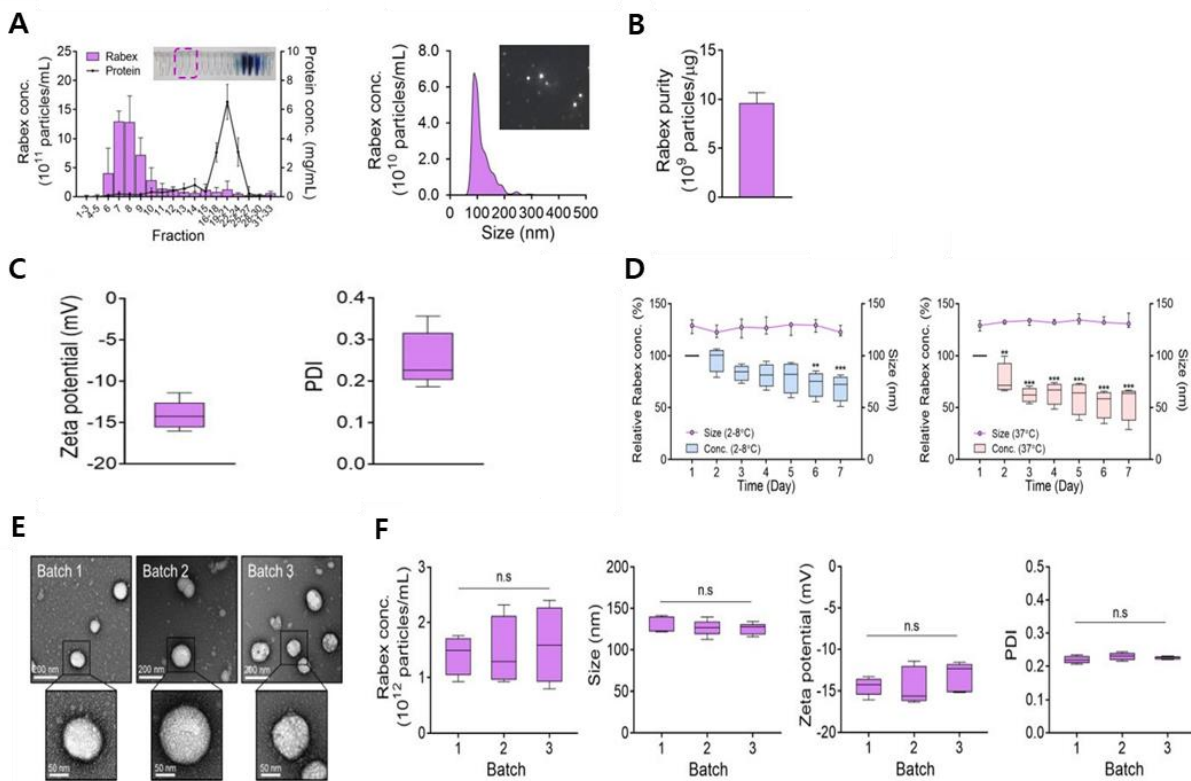


Figure 1. Isolation and characterization of Rabex. (A) EV fractional concentrations and protein impurity concentrations of Red cabbage juice after purification by size, exclusion chromatography and NTA for Rabex size and concentration assessments. (B) Purity (C) zeta potential and PDI (D) Investigation of temperature- and time-dependent Rabex stability at 2 – 8°C and 37°C in PBS solution.(E) TEM analysis of Rabex morphology among 3 different batches of Rabex, with size bars indicating 200 μ m (upper panel) and 50 μ m (lower panel), respectively. (F) Batch analysis of Rabex concentration, size, zeta potential, and PDI. The data are presented as mean \pm SEM, $n \geq 3$. Statistical significance is indicated as follows: * $p < 0.05$; ** $p < 0.01$; *** $p < 0.001$; n.s, not significant.

Cellular Uptake and Mechanism of Delivery

To evaluate cellular delivery, Rabex was labeled with PKH67 and incubated with Caco-2 cells. Confocal imaging demonstrated strong intracellular fluorescence, confirming cellular uptake (Figure 1H). Endocytosis inhibition assays revealed that Rabex uptake was significantly reduced when clathrin-mediated endocytosis or phagocytosis was blocked using chlorpromazine and cytochalasin D, respectively, whereas caveolin-mediated endocytosis and macropinocytosis had little effect (Figure 1I).

Rabex Enhances Skin-Relevant Cell Proliferation and Barrier Function

WST-1 assays in Caco-2 and THP-1 cells showed that Rabex enhanced proliferation in a dose-dependent manner, particularly at higher doses (1×10^{11} particles/mL), with no evidence of cytotoxicity (Figure 2A–D). In THP-1 macrophages, qRT-PCR demonstrated that Rabex

suppressed the LPS-induced expression of M1 markers TNF- α and IL-1 β by 49.8% and 74.9%, respectively (Figure 2E).

DCF-DA staining revealed that Rabex decreased ROS generation in both THP-1 and Caco-2 cells under inflammatory stimuli (Figure 2F). In DSS-treated Caco-2 cells, Rabex pretreatment significantly increased cell viability from 44.2% to 66.5% (Figure 2G). TEER values dropped to 56.7% following DSS exposure but were maintained at 89.7% when Rabex was applied, indicating preserved tight junction integrity (Figure 2H).

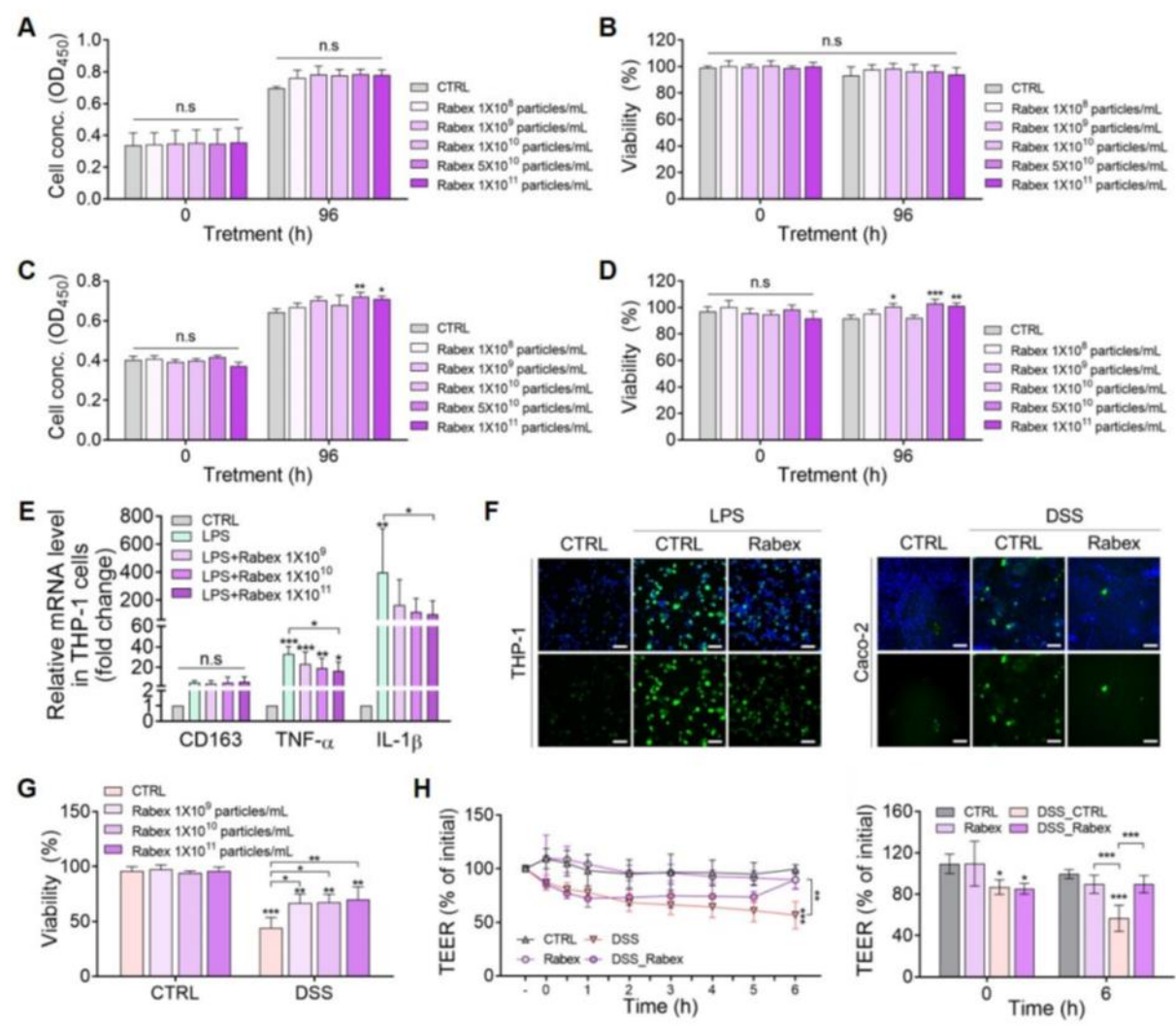


Figure 2. Regulation of macrophage inflammation and promotion of epithelial cell regeneration by Rabex. (A, B) Effect of Rabex on Caco-2 colon epithelial cell proliferation (A) and cytotoxicity (B). (C, D) Effect of Rabex on THP-1 macrophage proliferation (C) and cytotoxicity (D). Different concentrations of Rabex were administered to each cell line, and Rabex promoted the proliferation of both cell lines without exhibiting toxicity. (E) Dose-dependent inhibition of inflammation by Rabex in THP-1 cells treated with LPS. Cells were treated the LPS for the induction of inflammation in the absence or presence of Rabex. Anti-inflammatory effects were assessed using RT-PCR analysis of M1 polarization markers. (F) Antioxidative effect of Rabex was assessed in THP-1 and Caco-2 cells treated with LPS

and DSS, respectively, for ROS generation. ROS level was detected by DCF-DA staining, with size bars indicating 100 µm. (G) Inhibition of DSS-induced cell death in Caco-2 cells by Rabex. (H) Effect of Rabex on DSS-induced paracellular permeability as demonstrated by the impact of Rabex on the TEER of a Caco-2 cell monolayer. Rabex treatment was observed to prevent changes in TEER induced by DSS. The data are presented as mean \pm SEM, $n \geq 3$. Statistical significance is indicated as follows: * $p < 0.05$; ** $p < 0.01$; *** $p < 0.001$; n.s, not significant.

Surface Engineering of Rabex for Targeted Delivery (t-Rabex)

To enhance delivery to CD44-expressing cells (e.g., keratinocytes, immune cells), Rabex was modified with DSPE–PEG–HA. Conjugation was confirmed by ^1H -NMR and FT-IR (Figure 3A), and particle characterization by NTA and TEM showed no major size or shape changes (Figure 3B). Zeta potential shifted from -14.4 to -20.9 mV after HA modification (Figure 3C), while PDI remained consistent (Figure 3D).

In Caco-2 cells, t-Rabex uptake increased from 46.9% to 67.6%, and in THP-1 cells, from 29.9% to 57.8% (Figure 3E). CD44 receptor blocking reduced t-Rabex uptake by 14.5%, confirming CD44-dependent targeting (Figure 3F). Fluorescence microscopy revealed near-complete internalization of t-Rabex in THP-1 cells (Figure 3G). Importantly, t-Rabex promoted cell viability, showing no cytotoxicity and even enhancing proliferation at concentrations up to 2×10^{10} particles/mL (Figure 3H).

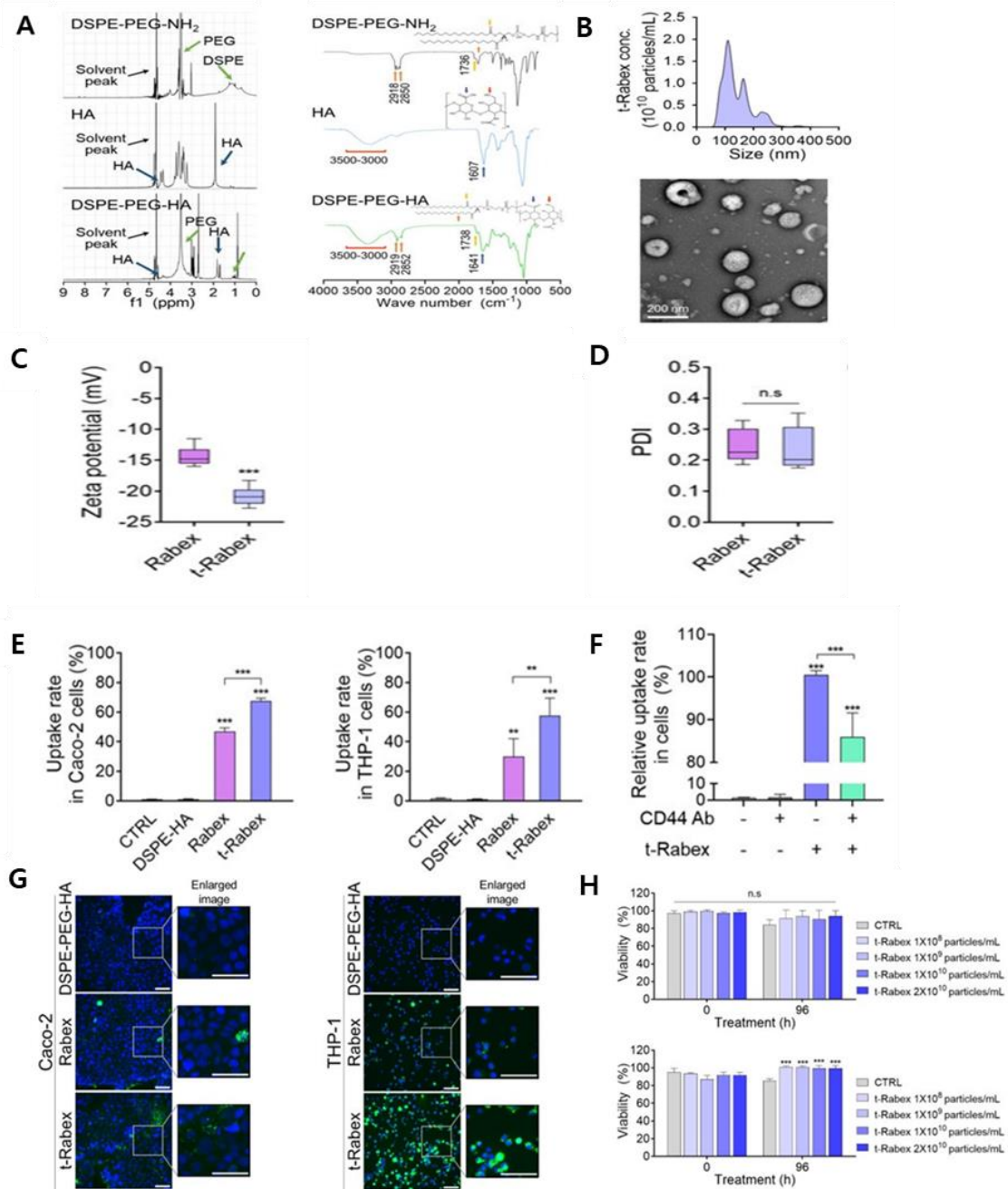


Figure 3. Surface engineering of Rabex to improve targeting efficiency (A) ^1H -NMR spectroscopy confirming DSPE-PEG-HA synthesis and highlighting HA and DSPE-PEG-NH₂ peaks. and FT-IR spectra of HA, DSPE, and DSPE-PEG-HA conjugate. Orange arrows: methylene groups of DSPE; Yellow arrows: carbonyl groups of DSPE; Red arrows: hydroxyl groups of HA and amine groups of DSPE; Blue arrows: carboxylic groups of HA. (B) Characterization of t-Rabex for their size and morphology (C) Zeta potential (D) PDI (E) Flow cytometric analysis demonstrating t-Rabex delivery to Caco-2 cells. Rabex and t-Rabex were stained with PKH staining dye, and DSPE-PEG-HA without Rabex was used as negative control. Note that a higher number of t-Rabex was taken up by colon epithelial cells compared to that of Rabex. and Flow cytometric analysis of t-Rabex in

*THP-1 cells indicating surface engineered t-Rabex exhibited enhanced cellular uptake in both cells. (F) The CD44 receptor targeting efficiency of t-Rabex was assessed using flow cytometry on THP-1 cells, both with and without the CD44 blocking antibody. (G) Fluorescent microscopy demonstrating the enhanced t-Rabex uptake into Caco-2 and THP-1 cells, with size bars indicating 100 µm. Free DSPE-PEG-HA without Rabex (upper panel), Rabex (middle panel), and t-Rabex (lower panel) were imaged for the comparison. (h) Assessment of cytotoxicity of t-Rabex using the WST-1 assay. Note that t-Rabex exhibited no cytotoxicity in Caco-2 and THP-1 cells. The data are presented as mean ± SEM, n ≥ 3. Statistical significance is indicated as follows: **p < 0.01; ***p < 0.001; n.s, not significant.*

4. Discussion

The comprehensive physicochemical and biological characterization of Rabex confirms its suitability as a bioactive nanocarrier for dermocosmetic use. The particle size, surface charge, stability in serum and PBS, and high reproducibility across production batches strongly support its potential for commercial development. Unlike mammalian EVs, Rabex is inexpensive and scalable, without sacrificing bioactivity or stability.

In vitro functional assays demonstrated that Rabex enhances epithelial and immune cell proliferation while mitigating inflammatory cytokine expression and oxidative stress. These are hallmark indicators of efficacy in skincare formulations targeting sensitive or inflamed skin conditions.

Furthermore, Rabex preserved epithelial barrier integrity under stress (DSS exposure), restoring TEER values and cell viability. These features make Rabex particularly promising for formulations aiming to restore or protect the skin barrier—a central concern in modern cosmetic science.

The addition of hyaluronic acid to create t-Rabex represents a strategic improvement for targeted action. HA binds CD44 receptors, commonly overexpressed in damaged or inflamed tissue. t-Rabex showed significantly enhanced cellular uptake, especially in THP-1 cells, and retained all beneficial properties of unmodified Rabex. The engineering approach allows delivery of a lower Rabex dose (1/10th) while achieving comparable or superior efficacy, presenting clear advantages in formulation cost and efficiency.

Taken together, Rabex and its engineered form, t-Rabex, exhibit multifunctional performance—anti-inflammatory, antioxidant, proliferative, and barrier-restorative—coupled with enhanced cell-targeting capability. These properties suggest strong potential for application in high-performance skincare products such as barrier creams, anti-aging serums, and post-procedure recovery formulas.

5. Conclusion

In this study, red cabbage-derived extracellular vesicles (Rabex) and their hyaluronic acid-modified derivative (t-Rabex) were successfully developed, characterized, and evaluated for their potential use in cosmetic applications. Rabex was consistently produced with high purity and reproducibility and displayed stable physicochemical properties in both aqueous and serum environments.

In vitro experiments demonstrated that Rabex significantly promoted keratinocyte and macrophage proliferation, suppressed pro-inflammatory cytokine expression, reduced oxidative stress, and preserved epithelial barrier integrity under inflammatory conditions. These multifunctional activities highlight Rabex as a potent bioactive for addressing common skin concerns such as inflammation, sensitivity, and barrier damage.

Furthermore, surface modification of Rabex with hyaluronic acid to generate t-Rabex effectively enhanced cellular uptake through CD44-targeted delivery, particularly in immune cells, without inducing cytotoxicity. t-Rabex maintained or improved bioactivity at a significantly lower dose than unmodified Rabex, providing a strategic advantage in formulation efficiency and targeted delivery.

Taken together, Rabex and t-Rabex present as promising next-generation plant-derived cosmetic actives with multifunctional efficacy—combining anti-inflammatory, antioxidant, barrier-reinforcing, and targeted delivery properties. Their scalability, safety, and biological activity support further development as novel nanovesicular carriers in advanced skincare formulations targeting sensitive, aging, or inflamed skin.

Reference

- [1]. Kang, S. J., Lee, J. H., & Rhee, W. J. (2024). Engineered plant-derived extracellular vesicles for targeted regulation and treatment of colitis-associated inflammation. *Theranostics*, 14(14), 5643–5661.
- [2]. You, J. Y., Kang, S. J., & Rhee, W. J. (2021). Isolation of cabbage exosome-like nanovesicles and investigation of their biological activities in human cells. *Bioactive Materials*, 6, 4321–4332.
- [3]. Huang R, Jia B, Su D, Li M, Xu Z, He C, et al. Plant exosomes fused with engineered mesenchymal stem cell-derived nanovesicles for synergistic therapy of autoimmune skin disorders. *J Extracell Vesicles*. 2023; 12: e12361.
- [4]. Mondal, J., Pillarisetti, S., Junnuthula, V., Saha, M., Hwang, S. R., Park, I. K., & Lee, Y. K. (2023). Hybrid exosomes, exosome-like nanovesicles and engineered exosomes for therapeutic applications. *Journal of Controlled Release*, 353, 1127–1149.